

Microcomputer Simulation of Solid-State ^{13}C NMR Line Shapes Affected by Quadrupolar Nuclei

Alejandro Olivieri,* Lucio Frydman, Mariano Grasselli and Luis Diaz

Facultad de Farmacia y Bioquímica, Universidad de Buenos Aires, Junin 956, Buenos Aires (1113), Argentina

Solid-state ^{13}C NMR spectra of ^{14}N -containing compounds obtained under CPMAS conditions often show asymmetric doublets arising from the unaveraged ^{13}C , ^{14}N residual dipolar coupling. A similar result has recently been noticed in deuteriated samples, whose ^{13}C resonances showed the combined effect of ^{13}C , ^2H dipolar and scalar couplings. A simple approach, easily adaptable to a desk microcomputer, is described for simulating ^{13}C line shapes for arbitrary values of quadrupole parameters, C—X ($\text{X} = ^{14}\text{N}$, ^2H) distances, external field and orientation of the internuclear vector in the axis system where the electric field gradient tensor is diagonal.

KEY WORDS Quadrupole effects in CPMAS spectra ^{13}C , ^{14}N and ^{13}C , ^2H residual dipolar coupling
 ^{13}C line shape simulation

INTRODUCTION

High-resolution solid-state ^{13}C NMR spectra of compounds containing quadrupolar nuclei such as ^{14}N show a characteristic deformation mainly observed as asymmetric doublets.¹⁻³ In recent years, considerable interest has been focused on the theoretical aspects involved in this phenomenon⁴⁻¹³ owing to the relevant information contained in these splittings. We have recently derived¹⁴ an analytical, first-order equation correlating the value of the splitting S with a number of variables, such as the quadrupole coupling constant of the quadrupolar nucleus $\chi = e^2 q_{zz} Q/h$, the asymmetry parameter η of the quadrupole tensor, the dipolar coupling constant $D = \gamma_C \gamma_N h/4\pi^2 r_{\text{CN}}^3$, the Zeeman frequency $Z_N = \gamma_N B_0/2\pi$ of the nitrogen nucleus in the applied external field and the Euler angles β^D and α^D which define the orientation of the internuclear vector \bar{r}_{CN} in the principal axis system (PAS) of the electric field gradient (EFG) at ^{14}N . This simple approach was found to reproduce experimental measurements of S with remarkable accuracy,¹⁴ and has also been successfully applied to the line shape simulation of ^{13}C CPMAS spectra of solid ribonucleosides.¹⁵ A similar effect has recently been reported in deuteriated glucose,¹⁶ although in this case the spectra showed the extra complication of the scalar ^{13}C , ^2H coupling. Since ^2H quadrupole coupling constants are generally an order of magnitude smaller than those of ^{14}N nuclei, our first-order perturbative approach should also give good results for deuteriated compounds, provided that the effect of $J(^{13}\text{C}, ^2\text{H})$ is taken into account. In this paper, we show how this method can be used to calculate the ^{13}C line shapes affected by the presence of ^{14}N or ^2H for arbitrary values of the geometric (β^D , α^D , r_{CX}) and

energetic (χ , η , Z_X) parameters involved ($\text{X} = ^{14}\text{N}$, ^2H). In contrast to previous studies, the simulation procedure described here can be easily implemented on a desk microcomputer.

RESULTS AND DISCUSSION

It is already known that the effect of ^{14}N nuclei on adjacent ^{13}C arises from the fact that the ^{14}N spin states are not quantized along the external field axis, owing to the presence of an EFG characterized by the values of χ and η . The resulting admixture of the Zeeman states $|+1\rangle$, $|0\rangle$ and $|-1\rangle$ leads to a dipolar ^{13}C , ^{14}N interaction which cannot be suppressed by MAS, producing a splitting of the ^{13}C resonance together with a characteristic broadening.¹⁴ Calling ν_i ($i = 1, 2, 3$) the first-order frequency shifts caused by each ^{14}N eigenstate ($|1\rangle \cong |+1\rangle$; $|2\rangle \cong |0\rangle$; $|3\rangle \cong |-1\rangle$), we previously derived the following equations:¹⁴

$$\nu_1 = -\nu_2/2 - D(1 - 3 \cos^2 \Omega) \quad (1a)$$

$$\nu_3 = -\nu_2/2 + D(1 - 3 \cos^2 \Omega) \quad (1b)$$

$$\begin{aligned} \nu_2 = & (3D\chi/2Z_N)[3(\cos \beta^D - \cos \theta \cos \Omega) \\ & \times \cos \theta \cos \Omega + \eta (\sin \beta^D \cos \alpha^D \\ & - \cos \delta \cos \Omega) \cos \delta \cos \Omega - \eta \\ & \times (\sin \beta^D \sin \alpha^D - \cos \varepsilon \cos \Omega) \\ & \times \cos \varepsilon \cos \Omega] \quad (1c) \end{aligned}$$

where δ , ε , θ and Ω are the polar angles defining the orientations of the principal axes x , y , z of the EFG tensor and of the internuclear vector \bar{r}_{CN} , respectively in the Zeeman frame.¹⁴ Since the term $(1 - 3 \cos^2 \Omega)$ vanishes with MAS, Eqns (1a)–(1c) show that the ν_1 and ν_3 lines will be coincident at a distance from the ^{13}C unperturbed frequency which is half that for the ν_2 line.

* Author to whom correspondence should be addressed. Present address: Department of Chemistry, University of Illinois at Urbana-Champaign, Urbana, IL 61801, USA.

This predicts an asymmetric splitting into two peaks of relative areas 2:1, whose magnitude can be given as a function of D , χ , η , Z_N , β^D and α^D .¹⁴

Equations (1a)–(1c) can be used to predict the powder patterns generated by this residual ^{13}C , ^{14}N dipolar coupling. To take into account the time dependence of the cosines due to the spinning about the magic axis, the following equations are introduced:

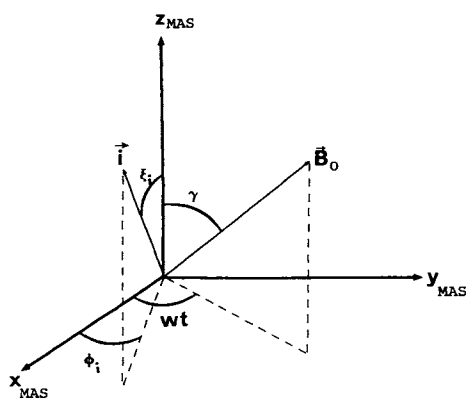
$$\cos \vartheta_i = \cos \gamma \cos \xi_i + \sin \gamma \sin \xi_i \times \cos (wt - \phi_i) \quad i = x, y, z, r \quad (2)$$

where we now use the notation $\delta = \vartheta_x$, $\varepsilon = \vartheta_y$, $\theta = \vartheta_z$, $\Omega = \vartheta_r$; ξ_i and ϕ_i are the polar and azimuth angles that define the orientations of the x , y , z axes of the PAS and \bar{r}_{CN} , respectively, with respect to the MAS frame (Fig. 1a), w is the spinning frequency and γ is the magic angle (54.7°).

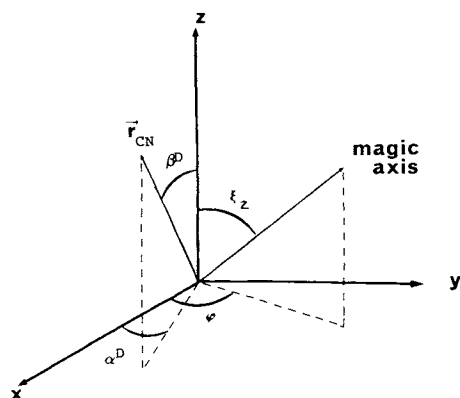
After replacing $\cos \vartheta_i$ taken from Eqn (2) in Eqns (1a)–(1c), a time averaging is performed; this is possible since the spinning frequencies commonly employed in conventional CPMAS equipments (3–5 kHz) are higher than the ^{13}C , ^{14}N dipolar interaction. The result is

$$v_1 = v_3 = -v_2/2 \quad (3a)$$

$$v_2 = (3D\chi/2Z_N) (\cos^2 \beta^D + \frac{1}{3}\eta \sin^2 \beta^D \times \cos 2\alpha^D - A/6 + \eta B/18) \quad (3b)$$



a



b

Figure 1. (a) Orientations of the external field B_0 , the principal axes x , y , z of the EFG tensor and the internuclear vector \bar{r}_{CN} in the MAS frame, where z_{MAS} is the spinning axis ($i = x, y, z, r$). (b) Orientation of the spinning axis and \bar{r}_{CN} in the PAS of the EFG tensor used to derive Eqns (4).

where

$$A = 1 + \cos^2 \xi_z + \cos^2 \xi_r - 9 \cos^2 \xi_x \times \cos^2 \xi_r + 2(\cos \beta^D + \cos \xi_z \cos \xi_r)^2 \quad (3c)$$

$$B = (\cos^2 \xi_y - \cos^2 \xi_x)(1 - 9 \cos^2 \xi_r) + 2(\sin \beta^D \sin \alpha^D + \cos \xi_y \cos \xi_r)^2 - 2(\sin \beta^D \cos \alpha^D + \cos \xi_x \cos \xi_r)^2 \quad (3d)$$

For fixed values of β^D , α^D , χ , η , D and Z_N , Eqns (3a)–(3d) are a function of the polar angles ξ_i . The latter are not completely independent, however, since the following equations relate $\cos \xi_r$, $\cos \xi_y$ and $\cos \xi_x$ with the angles ξ_z and φ which define the orientation of the spinning axis in the PAS of the EFG tensor (Fig. 1b):

$$\cos \xi_r = \cos \xi_z \cos \beta^D + \sin \xi_z \times \sin \beta^D \cos (\alpha^D - \varphi) \quad (4a)$$

$$\cos \xi_y = \sin \xi_z \sin \varphi \quad (4b)$$

$$\cos \xi_x = \sin \xi_z \cos \varphi \quad (4c)$$

Therefore, for each orientation given by ξ_z and φ , the frequencies v_1 , v_2 and v_3 can be calculated through Eqns (3) and (4). A two-dimensional grid of values of ξ_z and φ can be constructed to take into account the effect of all possible orientations in space, ranging from 0 to π for ξ_z and from 0 to 2π for φ . It is necessary to use a grid fine enough that a smooth sum is obtained. Each calculation is given a weight equal to $\sin \xi_z$, resulting in a characteristic powder pattern. Equivalently, the grid can be constructed from values of $\cos \xi_z$ (ranging from 1 to -1) and φ . Thousands of orientations are required to achieve convergence with this method. An alternative approach to this normal spherical tiling is the interpolation between grid points on the triangular faces of an octahedron.¹⁷ A convenient weighting function is used to account for the fact that different points in the grid are at different distances from the origin, and also subtend different solid angles.¹⁷ This method greatly reduces the number of orientations required for convergence, decreasing the total computation time to *ca* 5 min in our Sinclair QL microcomputer (a listing of the program is available on request).

Some representative line shapes are presented in Fig. 2, plotted using $(D\chi/Z_N)$ as a unit of frequency. These results are in good agreement with the band shapes reported in the literature, which were calculated by computer diagonalization of the full ^{14}N Hamiltonian (see, for instance, Figs 1 and 3 in Ref. 5 and Figs 2, 3, and 7 in Ref. 8). Also noticeable is the fact that the partition S , defined as the distance between the centres of gravity of the powder patterns v_2 and $v_{1,3}$, follows the behaviour traced by the previously reported equation:¹⁴

$$S = (9/20)(D\chi/Z_N) \times (3 \cos^2 \beta^D - 1 + \eta \sin^2 \beta^D \cos 2\alpha^D) \quad (5)$$

The effect of some of the parameters involved can be clearly appreciated through the use of Eqns (3) and (4). For example, when $\beta^D = 0$ (\bar{r}_{CN} collinear with z), Eqns (3) and (4) become independent of the angle α^D , in agreement with literature results.⁸ On the other hand, for axially symmetric EFG tensors, $\eta = 0$ and the depen-

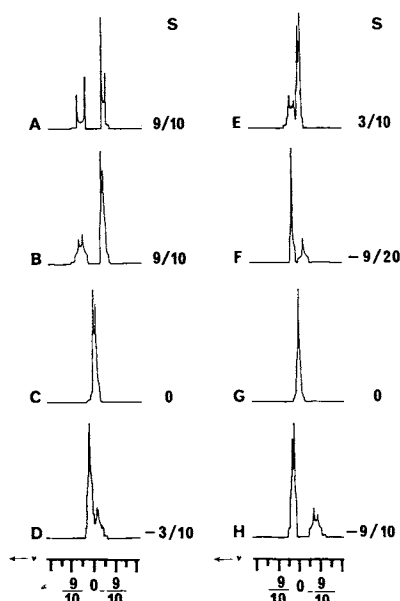


Figure 2. Calculated line shapes of ^{13}C affected by residual dipolar coupling to ^{14}N , using Eqns (3) and (4). An octahedral tiling scheme was used to account for all possible orientations in space. (A) $\beta^D = 0$, $\eta = 0$, $\alpha^D = 0$; (B) $\beta^D = 0$, $\eta = 1$, $\alpha^D = 0$; (C) $\beta^D = 54.7^\circ$, $\eta = 0$, $\alpha^D = 0$; (D) $\beta^D = 54.7^\circ$, $\eta = 1$, $\alpha^D = 90^\circ$; (E) $\beta^D = 54.7^\circ$, $\eta = 1$, $\alpha^D = 0$; (F) $\beta^D = 90^\circ$, $\eta = 0$, $\alpha^D = 0$; (G) $\beta^D = 90^\circ$, $\eta = 1$, $\alpha^D = 0$; (H) $\beta^D = 90^\circ$, $\eta = 1$, $\alpha^D = 90^\circ$. In all cases $D\chi/Z_N$ was chosen as the unit of frequency, the origin coinciding with the isotropic ^{13}C signal. Only representative values of β^D , α^D and η are used; the line shapes do not depend on the angle α^D when either $\beta^D = 0$ or $\eta = 0$. The value of the splitting S calculated with Eqn (5) is also given in each spectrum.

dence on α^D is only a phase shift added to φ . Since this latter angle is scanned in the range $0-2\pi$ to obtain the powder pattern, the line shape will be independent of α^D . This also agrees with previous reports showing that the effect of α^D is more pronounced as the value of η increases, the splitting S being independent of α^D for $\eta = 0$ ⁸ [see also Eqn (5)]. Finally, the effects of the values of D , χ and Z_N are simply interpreted as a scaling in the frequencies at which the powder patterns appear, through the combined factor $(D\chi/Z_N)$.

These considerations can also be extended to the ^{13}C , ^2H residual dipolar coupling, as recently seen in the case of α -D-glucose-1- d_1 ,¹⁶ provided that correct values of χ , η , $Z(^2\text{H}) = \gamma(^2\text{H})B_0/2\pi$ and $D(^{13}\text{C}, ^2\text{H})$ are used. The ^{13}C , ^2H scalar coupling should also be added in the form of its isotropic value J_{iso} , since quadrupole effects on this interaction can be neglected because $\chi(^2\text{H})/Z(^2\text{H}) \ll 1$.¹⁶ To take into account the scalar coupling effect, the lines ν_1 and ν_3 are shifted by $\pm J_{\text{iso}}$, resulting in the following new positions for the ^{13}C resonance:

$$\nu_1' = \nu_1 + J_{\text{iso}} \quad (6a)$$

$$\nu_2' = \nu_2 \quad (6b)$$

$$\nu_3' = \nu_3 - J_{\text{iso}} \quad (6c)$$

If one uses the values quoted in Ref. 16 [$\chi(^2\text{H}) = 188$ kHz, $D(^{13}\text{C}, ^2\text{H}) = 3.33$ kHz, $J_{\text{iso}} = 24.3$ Hz] and assumes an axially symmetric EFG collinear with the $^{13}\text{C}-^2\text{H}$ bond, the following calculations can be made either by using Eqn (5) or by computing the isotropic frequencies of the powder patterns generated by Eqns (6a)–(6c); at an external field of 4.7 T, the three average line positions for the ^{13}C resonances are +18.3 Hz (line 1'), +11.9 Hz (line 2') and -30.3 Hz (line 3'), where the origin is taken at the unperturbed ^{13}C chemical shift. This implies an overlapping of lines 1' and 2', leading to an expected splitting of ca 45 Hz (observed 46.8 Hz).¹⁶ Further, it also explains why the order of appearance of the peaks is reversed with respect to that expected if J_{iso} is not taken into account. As has been pointed out,¹⁶ the latter assumption would imply an unreasonable quadrupole coupling constant for the deuterium nucleus, which can now be estimated to be of the order of -500 kHz. On the other hand, at 1.32 T, Eqns (6a)–(6c) predict three peaks at +42.5 Hz (line 2'), +3.1 Hz (line 1') and -45.5 Hz (line 3'), whereas the experimental results show a downfield broad peak separated by 64 Hz from a small upfield peak.¹⁶ This could be in agreement with predicted line shapes if the assumption is made that peaks 2' and 1' are the constituents of the broad signal, which would then be centred at ca +23 Hz, suggesting a splitting of 68.5 Hz.

CONCLUSION

A procedure has been described which allows a successful simulation of ^{13}C NMR line shapes arising from residual dipolar coupling between ^{13}C nuclei and spin 1 quadrupolar nuclei such as ^{14}N and ^2H , based on a first-order perturbative approach. It can be easily adapted to a desk microcomputer program, providing the opportunity of simulating powder patterns with a success comparable to that obtained from more refined studies derived from computer diagonalization of the complete Zeeman-quadrupole Hamiltonian. This may prove useful in the interpretation of high-resolution solid-state ^{13}C NMR studies, particularly in those conducted at low fields.

Acknowledgments

This work was made possible through financial support from CONICET (Consejo Nacional de Investigaciones Científicas y Técnicas, Argentina). Fellowships from CONICET (A. C. O. and L. F.) and from the University of Buenos Aires (M. G.) are also gratefully acknowledged.

REFERENCES

1. S. J. Opella, M. H. Frey and T. A. Cross, *J. Am. Chem. Soc.* **101**, 5856 (1979).
2. C. L. Groombridge, R. K. Harris, K. J. Packer, B. J. Say and S. F. Tanner, *J. Chem. Soc., Chem. Commun.* **174** (1980).
3. M. H. Frey and S. J. Opella, *J. Chem. Soc., Chem. Commun.* **474** (1980).
4. A. Naito, S. Ganapathy and C. A. McDowell, *J. Chem. Phys.* **74**, 5393 (1981).
5. N. Zumbulyadis, P. M. Henrichs and R. H. Young, *J. Chem. Phys.* **75**, 1603 (1981).
6. J. G. Hexem, M. H. Frey and S. J. Opella, *J. Am. Chem. Soc.* **103**, 224 (1981).

7. S. J. Opella, J. G. Hexem, M. H. Frey and T. A. Cross, *Philos. Trans. R. Soc. London, Ser. A* **299**, 665 (1981).
8. J. G. Hexem, M. H. Frey and S. J. Opella, *J. Chem. Phys.* **77**, 3847 (1982).
9. A. Naito, S. Ganapathy and C. A. McDowell, *J. Magn. Reson.* **48**, 367 (1982).
10. J. Bohm, D. Fenzke and H. Pfeifer, *J. Magn. Reson.* **55**, 197 (1983).
11. R. K. Harris, P. Jonsen and K. J. Packer, *Org. Magn. Reson.* **22**, 784 (1984).
12. R. K. Harris, P. Jonsen and K. J. Packer, *Magn. Reson. Chem.* **23**, 565 (1985).
13. R. K. Harris, P. Jonsen, K. J. Packer and C. Campbell, *Magn. Reson. Chem.* **24**, 977 (1986).
14. A. C. Olivieri, L. Frydman and L. E. Diaz, *J. Magn. Reson.* **75**, 50 (1987).
15. A. C. Olivieri, L. Frydman, M. Grasselli and L. E. Diaz, *Magn. Reson. Chem.* **26**, 281 (1988).
16. S. D. Swanson, S. Ganapathy and R. G. Bryant, *J. Magn. Reson.* **73**, 239 (1987).
17. D. W. Alderman, M. S. Solum and D. M. Grant, *J. Chem. Phys.* **84**, 3717 (1986).